

## Characterisation of Cavitating Flow in Real-Size Optical Injectors for Additised and Renewable Diesel Blends

I.K. Karathanassis<sup>1,2,\*</sup>, J. Hwang<sup>2,3</sup>, P. Koukouvinis<sup>1,2</sup>, L. Pickett<sup>2</sup>, D. Spivey<sup>4</sup>, M. Gavaises<sup>1</sup>

<sup>1</sup> School of Mathematics, Computer Science and Engineering, City, University of London, Northampton Square, EC1V0HB London, UK

<sup>2</sup> Combustion Research Facility, Sandia National Laboratories, 7011 East Avenue, Livermore, CA 94550, USA

<sup>3</sup> Centre for Advanced Vehicular Systems (CAVS), Department of Mechanical Engineering, Mississippi State University, Starkville, Mississippi, MS 39762, USA

<sup>4</sup> Lubrizol European Research and Development Centre, Nether Lane, Hazelwood, DE56 4AN Derby, UK

**Abstract:** The present flow-visualisation study evaluates in a comparative manner the fuel-injection characteristics of a multicomponent diesel sample, the same reference fuel treated with a viscoelasticity-inducing agent (Quaternary Ammonium Salt), as well as a RME biodiesel blend. High-speed imaging of the cavitating flow arising in different real-size, optical-injector geometries and the respective near-nozzle spray evolution was performed using both diffuse and parallel light. Experiments were conducted in a sealed vessel for injection and ambient pressures of 700-900 bar and 1-20 bar, respectively. Either bulk thermophysical properties, as in the case of the RME sample, or distinct rheological behaviour, referring to the viscoelastic fuel, were found to have a measurable influence on the morphology of the two-phase flow arising within the injector layout.

**Keywords:** high-speed imaging, schlieren imaging, vorticity, viscoelastic effects, biofuels

### 1. Introduction

Internal-combustion engines will be the primary propulsion systems for heavy-duty vehicles at least for the next three decades, as, unlike passenger cars and light-duty counterparts, the penetration of electrification in the relevant market is expected to be of the order of 10% by 2050 [1]. Hence, near- to mid-term technological solutions need to be adopted, in order to enhance the efficiency of modern diesel engines, not only in terms of performance but also concerning emissions and resources-depletion potential. The incorporation of alternative and renewable fuels can contribute to these aspects, yet the effects of their rheological and thermophysical properties on fuel delivery and combustion must be explicitly identified.

The occurrence of cavitation in the internal flow path of high-pressure fuel injectors is linked to the degree of atomisation and dynamics of the expelled spray. A significant number of high-speed visualisation investigations are available in the literature elucidating the onset, development and collapse of transient cavitation in the micro-orifices of transparent replicas resembling single [2,3] and multi-hole injector layouts [4–6]. A multitude of conventional and renewable fuels have been examined under realistic operating conditions and injection pressures up to 1000 bar [7,8]. As a common practice, visualisation studies rely on Mie-scattering, either side-scatter or backlit imaging, to detect liquid vapour interphases, indicative of cavitation-bubbles generation in internal flows and liquid break up in spray flows [9].

The present work offers a comparative assessment of conventional, renewable and additised diesel samples to pinpoint the influence of either bulk thermophysical properties or distinct rheological behaviour on fuel-injection attributes. Diffuse backlit imaging is employed to identify in-nozzle vapour formation, while a novel micro-schlieren technique is applied to capture the extent and dynamics of vortical structures.

\* Corresponding Author: Ioannis K. Karathanassis, ioannis.karathanassis@city.ac.uk

# CAV2021

11<sup>th</sup> International Symposium on Cavitation  
May 10-13, 2021, Daejeon, Korea

## 2. Materials and Methods

Experiments were conducted in a sealed vessel allowing optical access along two directions with constant nitrogen flow to regulate ambient pressures within the range of 1-20 bar at room temperature. Fuel injections with pressures of 700-900 bar were performed by an ECN Spray C/D injector having its tip removed and fitted with different acrylic micro-orifices. Namely, a straight (Spray C) and a tapered (Spray D, K factor of 1.5) single-orifice tip, corresponding to injector geometries extensively employed by the ECN network [10], were evaluated with nominal nozzle diameters of 208  $\mu\text{m}$  and 189  $\mu\text{m}$ , respectively. Spray-D nozzle is hydro-eroded to produce a smooth curvature at its inlet, which, along with the cross-sectional tapering, tend to suppress cavitation onset. Concurrent Diffuse Backlight Illumination (DBI) and schlieren imaging in an orthogonal orientation were performed at 100,000 Hz to illustrate the topology and dynamics of in-nozzle vorticity and cavitation, as well as near-nozzle spray cone angle dynamics. A lens-type schlieren system was realised employing a set of plano-convex lenses on each side of the vessel to produce a parallel light beam and focus it on the subsequent knife-edge, respectively. A detailed description of the experimental and optical set-ups can be found in [11].

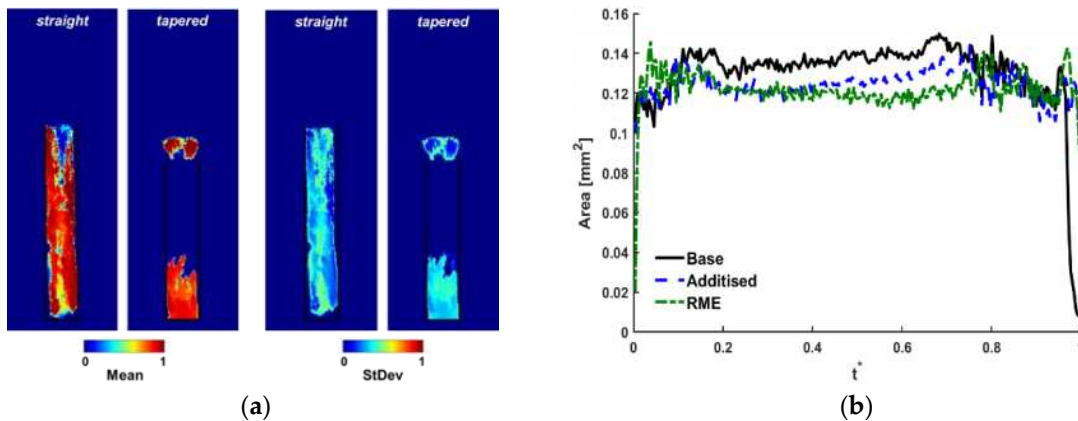
The post-processing treatment required to extract information with regard to in-nozzle cavitation from raw DBI images was based on a conventional thresholding and binarisation technique to identify the projected area of vaporous structures, owing to the refractive index gradient arising at interfaces. On the contrary, in-nozzle schlieren structures corresponding to longitudinal vortices produced weak contrast in the raw images, which required considerable enhancement and denoising, along with the application of the phase-congruency technique for detecting the edges of schlieren structures [11].

## 3. Results and Discussion

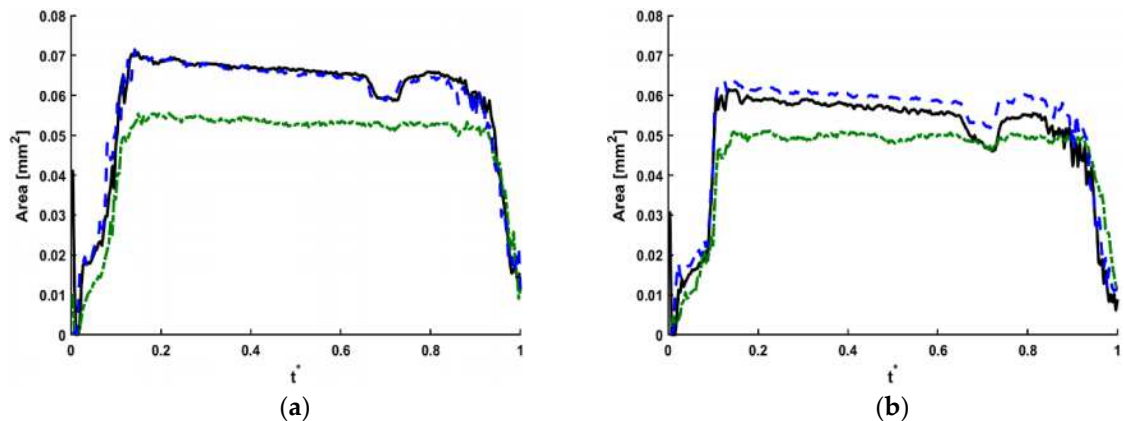
Indicative results derived from the flow-visualisation campaign are presented to reveal the differences detected between the reference diesel fuel, (QAS) additised and RME biodiesel examined. It should be noted that the base and RME biodiesel samples are characterised by thermophysical properties similar to commercial blends, whereas the addition of viscoelasticity-inducing agents has no effect on the bulk fuel properties. Figure 1a depicts contour plots of the mean vapour presence probability throughout the injection event and respective standard deviation for the Spray C and Spray D injectors, as derived by the DBI images. It is clearly evident that Spray C cavitates heavily with almost the entire orifice occupied by vapour, while vapour formation is much more moderate in the Spray D injector due to its tapered layout and hydro-grinded entrance. The standard-deviation plots reveal the existence of transient features, which are more localised in the Spray D layout. It must be noted that the Spray C nozzle is rendered fully opaque from cavitation for injection pressures higher than 700 bar. Figure 1b illustrates the distribution of vapour projected area with time for the C layout and demonstrates that the additised and RME samples exhibit deviations from the base fuel during the, so called, steady part of the injection with the biodiesel sample exhibiting the lowest values of projected area. In a similar manner, Figure 2 presents the same distribution, yet for the Spray D tip and different ambient conditions, while injection pressure is maintained at 900 bar. Once again, regardless of the ambient pressure, the RME sample exhibits the lowest projected-area values, a behaviour that should be attributed to its higher viscosity and thus reduced local Reynolds number in the orifice compared to the other two samples. It is interesting to notice that the additised sample shows a non-consistent trend compared to the reference diesel fuel. For a 5-bar ambient (Figure 2a) the two fuels have nearly identical distributions, whereas for a 20-bar ambient (Figure 2b, where the Cavitation Number actually decreases) the additised fuel obtains slightly, yet measurably higher values compared to base.

Figure 3a depicts the averaged presence probability of vortical structures within the nozzle throughout the duration of the injection event, as well as the respective standard deviation. It must be noted that schlieren imaging was performed in the mildly-cavitating Spray D injector, where optical access to the

nozzle could be attained. The probability contours plots clearly demonstrate the highly transient nature of the structures, in essence longitudinal vortices, as presence probability is of the order of 10%, while the standard-deviation plot indicates that structures forming in the sac region and in the vicinity of the needle tip, are subsequently entrained in the injector hole. Figure 3b quantifies the temporally-averaged projected area of vortical structures for different ambient conditions and fuel samples. The RME fuel exhibits the lowest values due to enhanced viscous damping of the structures. The additised sample obtains a comparable averaged value to the base diesel for 5-bar ambient, however it retains this value despite the increase of the ambient pressure, unlike the reference counterpart. It has been illustrated in previous experimental campaigns performed in enlarged injector replicas, refer indicatively to [12], that viscoelasticity effects tend to reduce the size of cross-flow vortices yet enhance that of longitudinal vortices, with subsequent after effects in the respective cavitation regimes (cloud or string cavitation). The combination of schlieren and diffuse-light imaging seems to demonstrate these effects in realistic injector layouts as well, since vapour extent is reduced (a consistent trend regardless of ambient pressure) in the fully cavitating Spray C injector for the viscoelastic sample, whereas increased vorticity in the D layout is postulated to be linked with the slight increase in the cavity projected area.



**Figure 1.** (a) Mean probability and standard deviation contour plots of vapour presence for the straight Spray C ( $p_{inj}=700/p_{amb}=5$  bar) and tapered D (900/5 bar) layouts. The black line indicates the outline of the injector-hole straight part; no cavities appear in the sac region. (b) Vapour projected-area distribution with time for Spray C (700/5 bar).  $t^*$  is the non-dimensional time normalised against the total injection duration.



**Figure 2.** Vapour projected area distribution with time for the Spray D injector: (a) 900/5 bar; (b) 900/20bar.

# CAV2021

11<sup>th</sup> International Symposium on Cavitation  
May 10-13, 2021, Daejeon, Korea

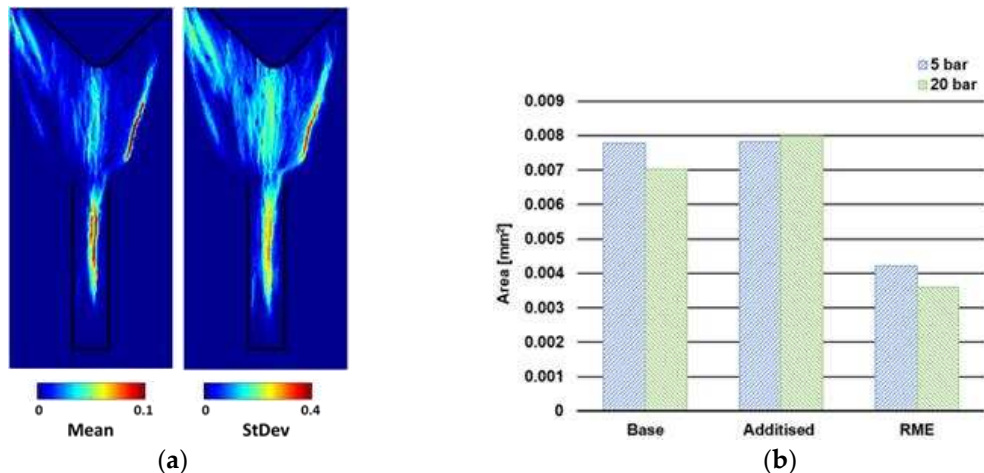


**Figure 3.** (a) Contour plots of vortical-structures mean presence probability and standard deviation in the Spray D injector (base fuel, 900/ 5 bar); (b) Temporally-averaged projected area of vortical structures for different ambient conditions.

**Acknowledgments:** Experiments were performed at the Combustion Research Facility, Sandia National Laboratories (SNL), a multi-mission laboratory managed and operated by National Technology and Engineering Solutions for Sandia LLC, a wholly owned subsidiary of Honeywell International, Inc., for the U.S. Department of Energy's National Nuclear Security Administration under contract DE-NA0003525. Funding from the EC Marie Skłodowska-Curie Global Fellowships AHEAD (IK, Grant No. 794831) and UNIFIED (PK, Grant No. 748784) is acknowledged, which also supported the international visiting program of I.K. Karathanassis and P. Koukouvinis at SNL.

## References

1. BloombergNEF, Electric Vehicle Outlook. Available online: [about.bnef.com/electric-vehicle-outlook/](https://about.bnef.com/electric-vehicle-outlook/) (accessed on 29 June 2020).
2. Kirsch, V.; Hermans, M.; Schönberger, J.; Ruoff, I.; Willmann, M.; Kneer, R.; Reddemann, M.A. Transparent high-pressure nozzles for visualization of nozzle internal and external flow. *Rev. Sci. Instrum.* **2019**, *90*, 033702.
3. Manin, J.; Pickett, L.M.; and Yasutomi, K. Stereoscopic high-speed microscopy to understand transient internal flow processes in high-pressure nozzles. *Exp. Therm. Fluid Sci.* **2020**, *114*, 110027.
4. Mitoglou, N.; McLorn, M.; Gavaises, M.; Soteriou, C.; Winterbourne, M. Instantaneous and ensemble average cavitation structures in Diesel micro-channel flow orifices. *Fuel* **2014**, *116*, 736–742.
5. Gold, M.; Pearson, R.; Turner, J.; Sykes, D.; Stetsyuk, V.; Sercey, G. et al. Simulation and measurement of transient fluid phenomena within diesel injection. *SAE Int. J. Adv. & Curr. Prac. in Mobility* **2019**, *1*, 291-305.
6. Yasutomi, K.; Hwang, J.; Pickett, L.M.; Sforzo, B.; Matusik, K.; Powell, C.F. Transient Internal Nozzle Flow in Transparent Multi-Hole Diesel Injector. *SAE Tech. Pap.* **2020**, 2020-01-08.
7. Payri, R.; Salvador, F.J.; Gimeno, J.; Venegas, O. Study of cavitation phenomenon using different fuels in a transparent nozzle by hydraulic characterization and visualization. *Exp. Therm. Fluid Sci.* **2013**, *44*, 235–244.
8. Jiang, G.; Zhang, Y.; Wen, H.; Xiao, G. Study of the generated density of cavitation inside diesel nozzle using different fuels and nozzles. *Energy Convers. Manag.* **2015**, *103*, 208–217.
9. Westlye, F.R.; Penney, K.; Ivarsson, A.; Pickett, L.M.; Manin, J.; Skeen, S.A. Diffuse back-illumination setup for high temporally resolved extinction imaging. *Appl. Opt.* **2017**, *56*, 5028.
10. ECN Network, [ecn.sandia.gov/diesel-spray-combustion/target-condition/spray-d-nozzle-geometry/](https://ecn.sandia.gov/diesel-spray-combustion/target-condition/spray-d-nozzle-geometry/)
11. Karathanassis, I.K.; Hwang, J.; Koukouvinis, P.; Pickett, L.; Gavaises, M. Combined visualisation of cavitation and vortical structures in a real - size optical diesel injector. *Exp. Fluids* **2021**, *62*, 1–18.
12. Karathanassis, I.K.; Trickett, K.; Koukouvinis, P.; Wang, J.; Barbour, R.; Gavaises, M. Illustrating the effect of viscoelastic additives on cavitation and turbulence with X-ray imaging. *Sci. Rep.* **2018**, *8*, 1–15.